

The fabrication of ordered nanoporous metal films based on high field anodic alumina and their selected transmission enhancement

Zhiwei Yao¹, Maojun Zheng^{1,3}, Li Ma² and Wenzhong Shen¹

¹ Laboratory of Condensed Matter Spectroscopy and Opto-Electronic Physics, Department of Physics, Shanghai Jiao Tong University, Shanghai 200240, People's Republic of China

² School of Chemistry and Chemical Technology, Shanghai Jiao Tong University, Shanghai 200240, People's Republic of China

E-mail: mjzheng@sjtu.edu.cn

Received 22 June 2008, in final form 20 September 2008

Published 22 October 2008

Online at stacks.iop.org/Nano/19/465705

Abstract

A two-step high field anodization and a controllable barrier layer removing process have been used for the fabrication of porous anodic alumina (PAA) with different morphologies. Based on the PAAs, porous noble metal films with widely tunable pore size and inter-pore distance have been realized by a simple sputtering method. Their morphology and optical properties were studied with a field-emission scanning electron microscope, and ultraviolet and ultraviolet–visible spectrophotometers. An enhanced light transmission of the nanoporous metal films was detected. The transmissivity of a normal incidence light can be enhanced over ten times within a certain selected wavelength range. The intensity and position of the transmission peak depend on the morphology and porosity of the metal films.

(Some figures in this article are in colour only in the electronic version)

1. Introduction

An enhanced light transmission of thin porous metal films was reported by Ebbesen in 1998 [1]. It mainly results from the surface plasmon polariton (SPP) in the metal film with ordered nanopore arrays [2]. Because of its special properties, such as high sensitivity and quick response to environmental change, the SPP has an advantage in sensor devices such as special toxic gas detection [3–5], optical application in waveguides [6], nanophotonics and optical electronic devices [7]. SPPs can be stimulated only in the same scale as the wavelength of the incident light, and the enhanced transmission spectrum strongly depends on the geometrical symmetry and morphology of the porous metal film.

Many methods have been used to prepare such thin porous metal films, including electrochemical processes, thermal decomposition of Au₂O₃, alloy deposition, chemical

etching, and the water-in-oil emulsion-induced micelles method [8–11]. The use of porous anodic alumina (PAA) as a template is a convenient method to fabricate nanostructure materials [12–14]. A porous metal film can be obtained by simply depositing metal on the PAA templates. Compared with other methods, it has several advantages such as low cost and easy controllability. Metal films with highly ordered pore arrays are realized by the PAA template method.

In this study, a two-step high field anodization process has been used to form the PAAs nanopore array [15–18]. It has a much wider range of pore size and inter-pore distance [19]. Because of its high efficiency, the anodization time can be greatly reduced compared with the traditional anodization method, from dozens of hours to minutes. Furthermore, the pore size can be expanded by acid solution etching, which is controllable by varying the etching time at a certain temperature.

One layer of thin noble metal film was deposited on the PAA nanopore arrays by simple metal sputtering. It was found

³ Author to whom any correspondence should be addressed.

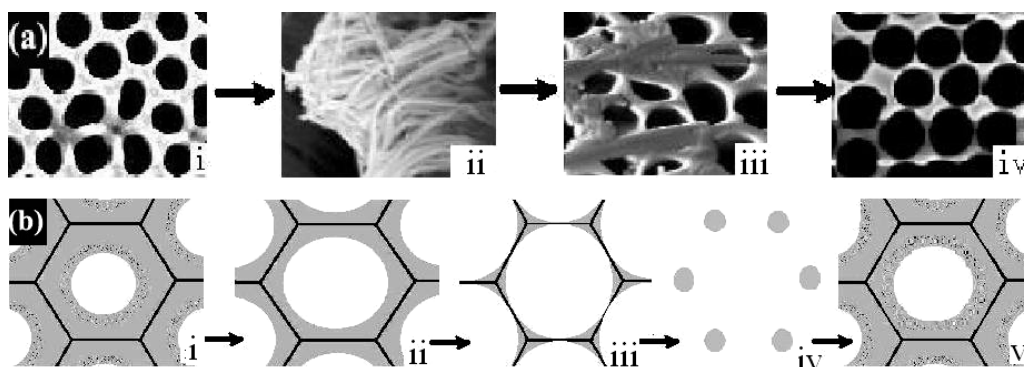


Figure 1. FE-SEM images and sketches of samples in different etching periods: (a) the FE-SEM images with etching time: (i) 10 min, (ii) 20 min, (iii) 30 min and (iv) 40 min; (b) schematics of a period during which the nanopores break down, nanowires form, the nanowires dissolve and nanopores appear again.

that there is an enhanced light transmission of the nanoporous metal film in the visible light range. The morphology and porosity of the porous metal film determine the intensity and peak position of the enhanced transmission spectrum.

2. Experimental details

The experiments consist of three main parts: the formation of PAA nanopore arrays, the deposition of the thin metal film, and the study of its optical properties.

2.1. The formation of PAA templates

A sheet of aluminum (99.999% purity, 0.25 mm thickness) was cut into many circular foils with a radius of 1 cm, degreased in acetone, washed in deionized water, and dried off by nitrogen gas. Then the circular foils were put into a special holder such that only a circular area of about 2 cm² was exposed to the electrolyte. Before anodization, the aluminum was electropolished at a constant voltage in a solution mixture of perchloric acid and ethanol (HClO₄:C₂H₅OH = 1:4 v/v) for several minutes to improve the smoothness of the surface.

To form a variety of PAAs we chose both the usual anodization and the high field method. The temperatures of the electrolytes were kept at -10 to 0 °C. The electrolytes (C₂H₅OH:H₂O = 1:4 v/v) can be oxalic acid (0.3 M) or H₃PO₄ (0.4 M) in the high field case. The first anodization step lasted for 2 h (for the usual case) or several minutes (for the high field case) to form hexagonal pore arrays. Then the foils were taken out and put into a mixture of 6 wt% phosphoric acid and 1.8 wt% chromic acid at a temperature of 60 °C to dissolve the orderless surface. After a second anodization with the same conditions as the first anodization, the nanopore arrays formed are highly uniform, in contrast to the former ones. The anodization time determines the depth of the pores.

The PAA templates were put into saturated CuSO₄ solution mixed with HCl (CuSO₄:HCl = 4:1 v/v) to remove all the Al layer. To remove the Al₂O₃ barrier layer, the samples were etched in 5% H₃PO₄ solution at a temperature of 35–45 °C for 30–45 min. The back layer of the PAA has more homogeneously distributed pores compared to the front side.

2.2. Deposition of metal film

One layer of Au was deposited perpendicularly on the back of the PAA by plasma sputtering (the atmospheric pressure was under 20 Pa, the ion current intensity was about 1 mA, the deposition rate of Au was about 2.0 nm min⁻¹, and the deposition time was 5 min). The thickness of the Au layer was fixed at about 10 nm for all samples. We also tried depositing a Ag layer by magnetron sputtering to compare with the Au ones.

2.3. Characterization

A field-emission scanning electron microscope (FE-SEM, Philips Sirion 200) was used to observe the morphology of the surface of the samples. Ultraviolet (Jobin Yvon THR1000, France) and ultraviolet–visible (LAMBDA 20/2.0, America) spectrophotometer systems were employed to detect the transmission spectra of the samples. The incident light is transmitted perpendicularly onto the surface of the samples.

3. Results and discussion

3.1. Morphology

By adjusting the anodization voltage and barrier layer etching progress, we realized a variety of samples with different inter-pore distances and pore diameters. The morphology of the front layer and the back layer were studied with the FE-SEM.

Figure 1(a) shows the FE-SEM images of the front layer of the PAAs with different etching time (10 min interval each). We can see that pore size expanded until the PAA cells broke down, with only alumina at the trigonal node left; thus nanowires were formed. Due to the influence of the outer field (mainly gravity field), the nanowires formed collapsed and a taper structure was formed (figure 1(a) (ii)). As the progress went on, the nanowires dissolved and the next layer of nanopores was exposed (figure 1(a) (iii–iv)). Figure 1(b) is sketch of the period during which the nanopores broke down, nanowires formed, the nanowires dissolved and then nanopores appeared again.

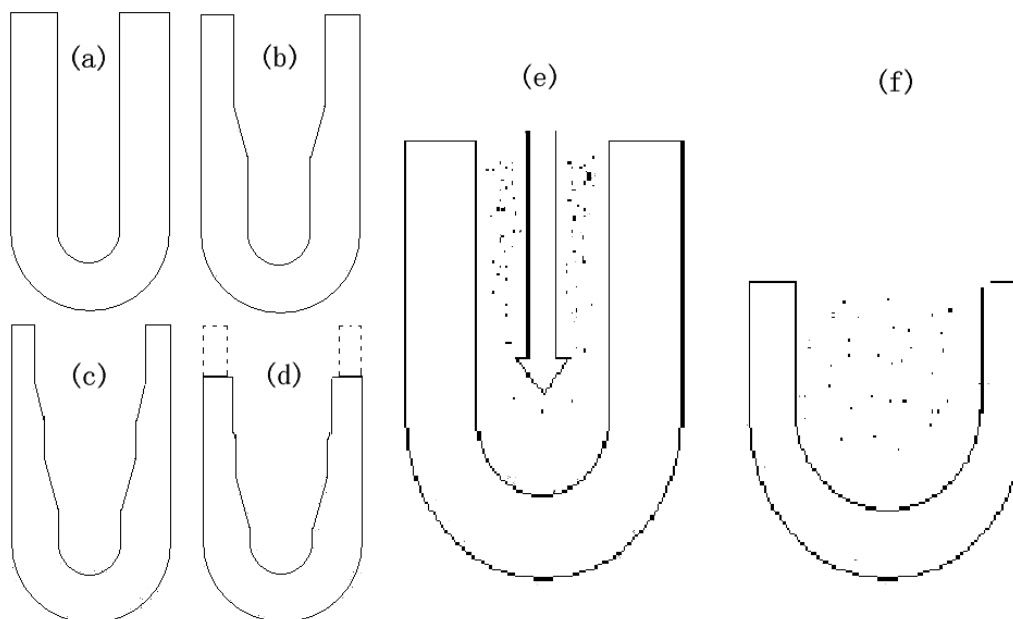


Figure 2. Sketches of the special etching progress: ((a)–(d)) nanowires form, segment by segment; (e) the acid concentration is lower at the bottom of the pore, where the arrow points; (f) the acid concentration becomes homogeneous as the pore size expands.

The morphology evolution characteristics in the etching progress can result from the concentration gradient of the acid solution in the nanohole. Figure 2 is a sketch of the PAA cells etched by the acid solution. For a faster supply rate, the concentration of acid solution around the surface could be higher than that at the bottom of the nanohole (figure 2(e)); thus the alumina at the top dissolves more quickly than that at the bottom [20]. So nanowires form segment by segment. As the upper segment dissolves, the next segment of nanowires is forming (figures 2(a)–(d)). The thickness of the nanopore PAA film decreases after one segment of nanowires is totally dissolved, which answers the doubt in some early studies [21]. Finally the whole part is dissolved after a long etching time. It is noted that the height or aspect ratio of the pores should play an important role in the concentration gradient inside the nanohole. The height of the nanohole can be over several micrometers, and this is mainly determined by the anodization time, while the pore size ranges from dozens to hundreds of nanometers and is mainly determined by the anodization voltage and etching progress. The nanoholes have a high aspect ratio, which can be over 50 (over 5 μm in height and about 100 nm in diameter). Probably, gradual pore widening is observed in high and narrow pores.

Figure 3 shows the SEM images of the back of the samples with different etching times. Before the barrier layer etching (the whole Al layer has been removed), its surface seemed like hexagonal ball arrays (figure 3(a)). The pores gradually appeared on the top of these balls (figures 3(b)–(d), 10 min interval each), then ordered nanopore arrays formed (figures 3(e)–(h)). We can see from the figures that the interpore distance of the samples is about 120 nm (figures 3(e), (f)) or 240 nm (figures 3(g), (h), high field case), and the pore size is about 50 nm (figures 3(e), (f)) or 120 nm (figures 3(g), (h), high field case).

Table 1. A series of pore sizes in different periods of etching the barrier layer at a temperature of 45 °C (units nm).

Anodization voltage (V)	Etching time (min)			
	10	20	30	40
120 (front layer, 0.3 M oxalic acid)	200	210	Null ^a	230
120 (back layer, 0.3 M oxalic acid)	115	155	195	Null ^b
140 (front layer, 0.3 M oxalic acid)	135	Null ^a	220	Null ^a
140 (back layer, 0.3 M oxalic acid)	90	135	170	210
195 (front layer, 0.4 M phosphoric acid)	115	155	180	220
195 (back layer, 0.4 M phosphoric acid)	85	125	150	190

^a The hexagonal structure was destroyed and nanowires formed.

^b The nanostructure was totally etched.

The pore sizes of a series of samples are summarized in table 1. Generally, the pore size expanded as the samples were etched in the acid solution. When the nanopores were broken down by the acid solution etching, nanowires formed. At this time pore size data do not exist, marked as Null^a in table 1. After a long time etching, all the PAA cells were dissolved. Thus pore size data do not exist either, marked as Null^b in table 1.

We can see clearly the change of the expansion rate of pore sizes from table 1. The expansion rate of the pore size is fast in the beginning period. It becomes slower during the middle period. The change of the expansion rate of pore size can be explained by the layer structure of the PAA cell and the impurity distribution in the cell. Figure 4 shows an SEM

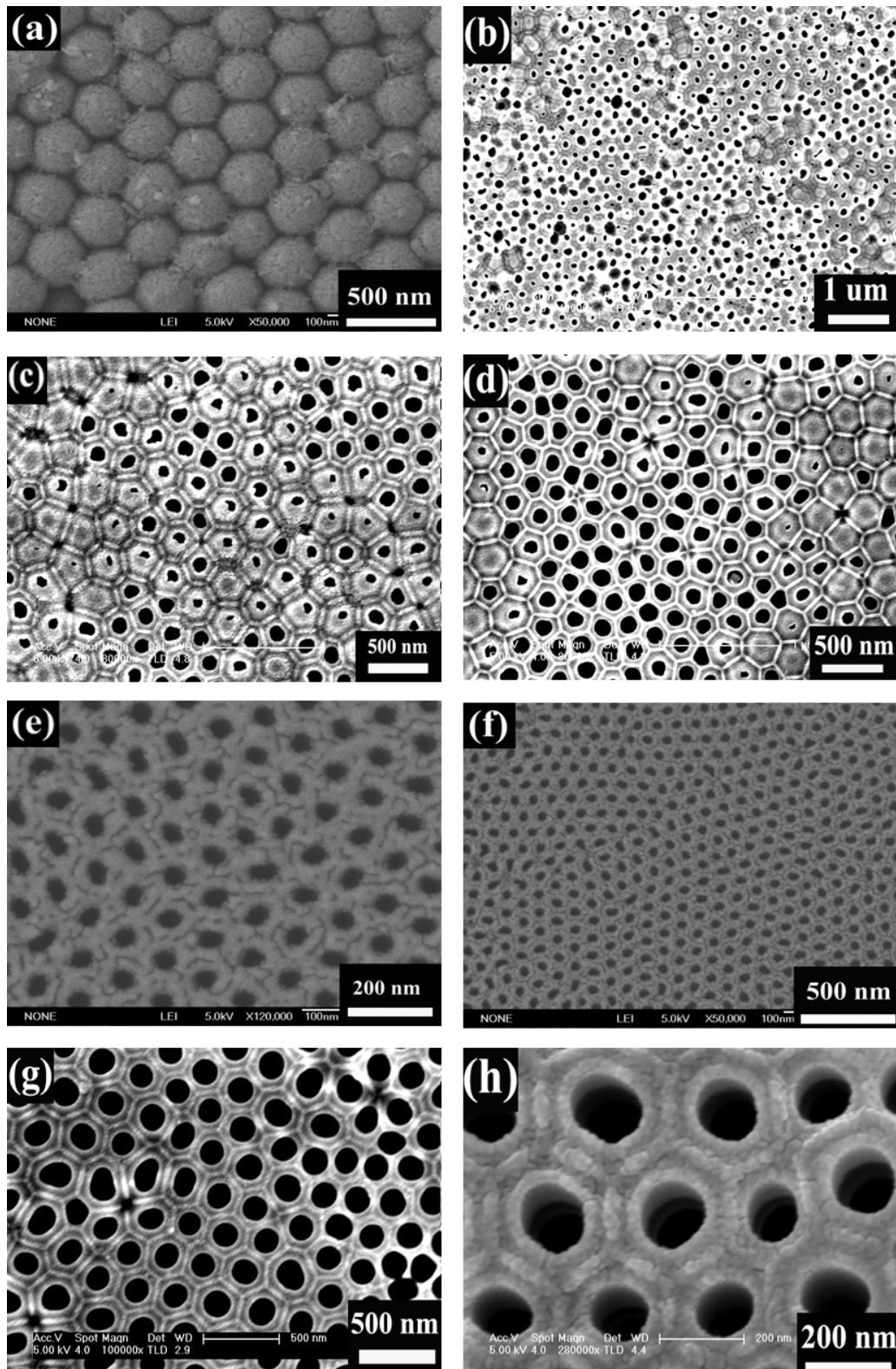


Figure 3. FE-SEM images of the back of samples: (a) back of barrier layer; ((b)–(d)) barrier layer partly removed with different etching time; ((e), (f)) anodization voltage $U = 40$ V, anodization time 8.5 h; ((g), (h)) $U = 140$ V, anodization time 5 min.

image of the PAA cell structure and an impurity distribution sketch diagram. Some research groups have reported that the hexagonal PAA cell is not homogeneous: it consists of a pure alumina inner layer and an outer layer with negative

ion impurities [22]. Impurities such as O^{2-} , OH^- , PO_4^{3-} , and $C_2O_4^{2-}$ are introduced during the anodization process. Further study has shown that most of the impurities are distributed in the intermediate part of the outer layer [23]. As the impurities

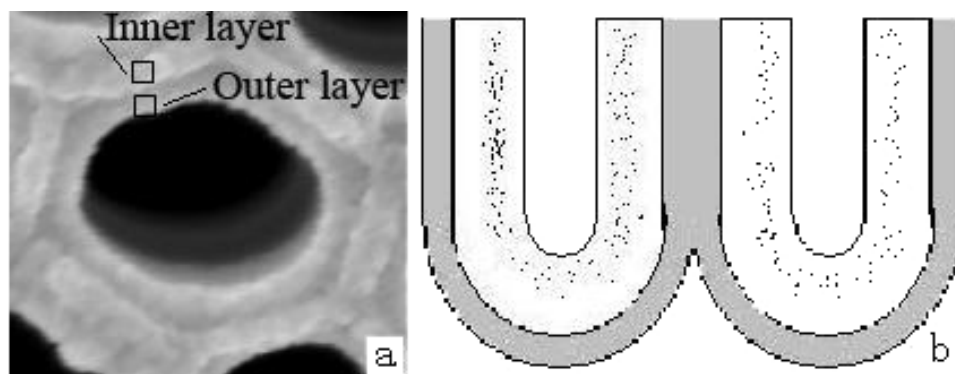


Figure 4. FE-SEM image and sketch of the PAA cell structure: (a) FE-SEM image of the hexagonal structure of a PAA cell, with an inner layer and an outer layer; (b) sketch of the layer structure of the PAA cell. The gray part is the pure alumina inner layer, while the white part is the outer layer with impurities (black dots) in its intermediate part.

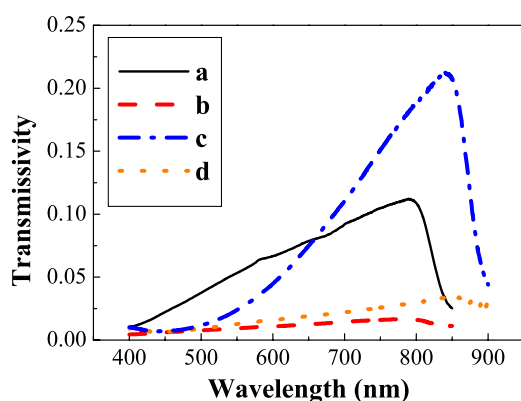


Figure 5. Transmission spectra of samples with barrier layer: (a) PAA ($U = 195$ V); (b) Au film on barrier layer surface of PAA ($U = 195$ V); (c) PAA ($U = 140$ V); (d) Au film on barrier layer surface of PAA ($U = 140$ V).

are distributed unevenly in the outer part, the etching speed in different parts will be correspondingly different. It is also found that the pore expansion rate increases again in the last etching period. The pore expansion contributes to the quick dispersion of the acid ions; thus more acid ions can be in contact with the pure alumina. So the speed increases again later.

In conclusion, the pore size can be adjusted by changing the etching time in 5% H_3PO_4 solution at a certain temperature. The inter-pore distance (D_{int}) can be adjusted by changing the anodization voltage (U). So, different morphologies of samples can be realized, as originally intended.

3.2. Transmission spectra

Figure 5 shows the transmission spectra of the samples with a barrier layer. A transmission peak around 800 nm (curve (a)) and 840 nm (curve (c)) is caused by the PAA templates fabricated at 195 and 140 V, respectively. After Au films were deposited on the barrier layer surface of PAAs, the transmissivity (curve (b), (d)) decreases significantly because the dense Au film on the barrier layer surface of the PAA

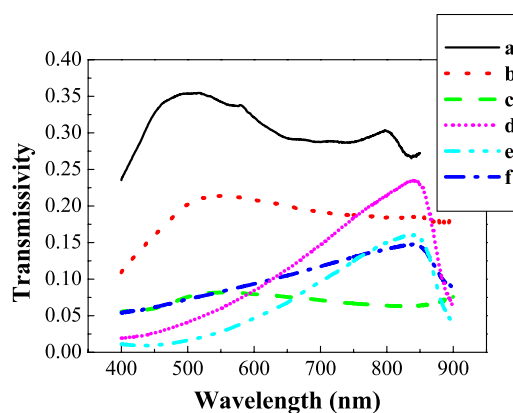


Figure 6. Transmission spectra of nanoporous samples without barrier layer: (a) Au film on PAA membrane ($U = 195$ V, 0.4 M phosphoric acid), porosity = 0.528 (etching temperature 45 °C, etching time 45 min); (b) Au film on PAA membrane ($U = 140$ V, 0.3 M oxalic acid), porosity = 0.344 (etching temperature 35 °C, etching time 40 min); (c) Au film on PAA membrane ($U = 140$ V, 0.3 M oxalic acid), porosity = 0.204 (etching temperature 35 °C, etching time 20 min); (d) PAA film, porosity = 0.528, $U = 195$ V; (e) PAA film, porosity = 0.344, $U = 140$ V; (f) PAA film, porosity = 0.204, $U = 140$ V.

has blocked off most of the incident light. However, the transmission peak positions do not change evidently, which indicates that there is no new physical mechanism occurring for usual dense Au film, or if an SPP is released, it is too weak to be detected.

When all the barrier layer was removed and pore arrays were exposed, deposition took place at the back side of the porous alumina film. In this case, the Au deposited only on the alumina areas between the pores. So the nanoporous Au film was formed on the surface of the PAA. Then SPPs can be detected with a clear enhanced transmission peak, as figure 6 shows. It can be seen that a new transmission peak (curve (a), (b) and (c)) appeared in the visible light range for all spectra of nanoporous Au films on the PAAs, which is markedly different from that (curve (d), (e) and (f)) of pure PAA membrane. This enhanced transmission peak could be stimulated by the SPPs in the nanoporous Au layer. Metals with nanostructure

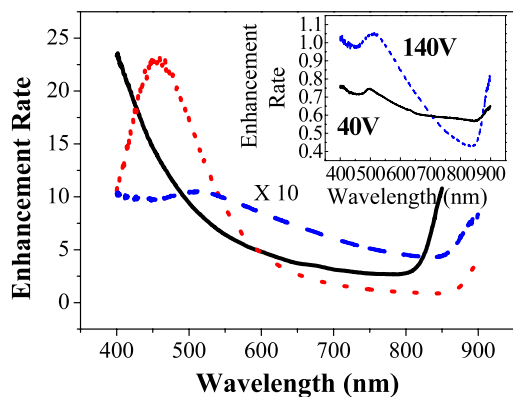


Figure 7. The transmission enhancement rate, intensity of Au film on porous PAA/intensity of bare PAA without barrier layer. Dotted line: $U = 140$ V, porosity 0.344; solid line: $U = 195$ V, porosity 0.528; dashed line ($\times 10$): $U = 140$ V, porosity 0.204; inset figure: solid line ($U = 40$ V, porosity 0.210), dashed line ($U = 140$ V, porosity 0.204).

can also be considered as photonic bandgap materials when light couples with surface plasmons (SPs) in transmission gratings. At the band edges, the SPP mode dispersion is flat and the associated density of SP modes is high, corresponding to a high field enhancement near the metal surface. The diffraction/interference light caused by the pore arrays also contributes to the transmission enhancement [1, 2, 24].

Actually the enhanced transmission peak gradually appears during the process of barrier layer etching. This means that the transmission enhancement effect stimulated by SPPs can occur when the porosity is above a critical value [25]. We consider the porous film as ideal hexagonal pore arrays, and thus we obtain the porosity of the metal films. The porosity of sample a (curve (a)) and b (curve (b)) is 0.528 and 0.344, respectively. Both of their spectra show a clear enhanced transmission peak, while a weak transmission peak (curve (c)) was detected for sample c with lower porosity of 0.204, which supports the discussion above. The SPPs in nanoporous metal films follow the electromagnetic (EM) field theory through certain boundary conditions [26]. In our study, the periodical nanopores are hexagonal, not rectangular, as another paper shows [27]. However, when the inter-pore distance of the pore is fixed, the main factor that influences the SPPs is the porosity.

It is noted that the new transmission peak positions (546 nm) of curves (b) (anodization voltage 140 V and porosity 0.344) and (c) (anodization voltage 140 V and porosity 0.204) are the same, while their intensities are quite different. Here, all Au films have the same thickness (about 10 nm). This implies that the transmission peak intensity depends on the pore size under the same inter-pore distance. However, the peak position (525 nm) of curve (a) (anodization voltage 195 V, porosity 0.528) is obviously different from that of curves (b) and (c). It can be deduced that the enhanced transmission peak position is mainly determined by the inter-pore distance of nanoporous Au films.

Figure 7 shows the transmission enhancement rate of these samples. The enhancement rate can be over ten times and it changes acutely within the wavelength range 450–550 nm

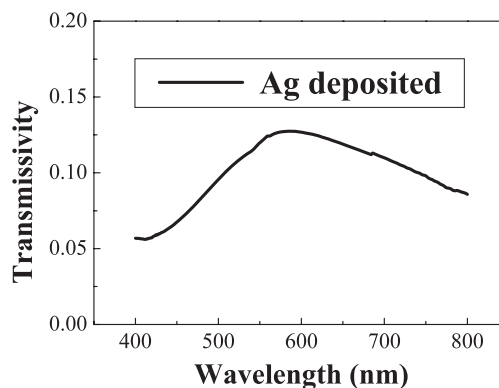


Figure 8. Transmission spectrum of Ag on nanoporous PAA ($U = 140$ V).

(solid line) for the sample with anodization voltage 195 V and porosity 0.528. The enhancement rate is also over ten times in the wavelength range 400–550 nm (dotted line) for the sample with anodization voltage 140 V and porosity 0.344. A sharp peak in this enhancement rate curve (dotted line) is also observed. The remarkable rate change indicates that the transmission enhancement effect of these two samples has a high sensitivity to the wavelength change. In contrast, the enhancement rate of the sample with anodization voltage 140 V and porosity 0.204 is only slightly higher than unity in a very narrow wavelength range (473–543 nm, dashed line). This shows that when the inter-pore distance is the same (dotted and dashed lines), the transmission enhancement effect is stronger for the higher porosity sample. For further investigation of the relation between the transmission enhancement rate and inter-pore distance under the same porosity, we examined the enhancement rate of the sample with anodization voltage 40 V (inter-pore distance 120 nm) and porosity 0.210, as shown in the inset (solid line) of figure 7. It is noted that the enhancement rate is less than unity in the whole wavelength range 400–900 nm. No enhancement effect is observed. The transmission enhancement rate of the sample with anodization voltage 140 V, inter-pore distance 240 nm and porosity 0.204 is also shown in this inset (dashed line) for comparison. The rate curves in the inset indicate that the transmission enhancement effect weakens with decreasing inter-pore distance under the same porosity.

Figure 8 shows the transmission spectrum of the sample with a Ag layer deposited. The anodization voltage of the PAA is 140 V, and the porosity of the nanoporous metal film is 0.344. The transmissivity is weak but a clear peak can be detected around 587 nm. So the peak position is also determined by the kind of metal deposited on the PAA templates.

4. Conclusion

A variety of PAAs with different sizes of inter-pore distance and pore diameter have been fabricated. After deposition of Au or Ag on PAAs we obtained ordered nanoporous metal films. An enhanced transmission peak caused by SPPs can be detected for samples without a barrier layer, which is

determined by porosity. A peak at 525 (546) nm is detected in the case of a nanoporous Au layer (587 nm for Ag), which shows that the enhanced transmission peak can be determined by the morphology of the porous metal film and the kind of metal deposited on the PAAs. Within a certain wavelength range the transmission enhancement rate can be over ten times, which implies that these nanoporous metal films have a high sensitivity to the wavelength change.

Acknowledgments

This work was supported by the Natural Science Foundation of China (grant No. 50572064), National Minister of Education Program of IRT0524 and National Major Basic Research Project of 2006CB921507. We thank the Instrumental Analysis Center of SJTU for use of the SEM facility.

References

- [1] Ebbesen T W, Lezec H J, Ghaemi H F, Thio T and Wolff P A 1998 *Nature* **391** 667
- [2] Barnes W L, Dereux A and Ebbesen T W 2003 *Nature* **424** 824
- [3] Liedberg B, Nylander C and Lundstrom I 1983 *Sensors Actuators* **4** 299
- [4] Samoylov A V, Mirsky V M, Hao Q, Swart C, Shirshov Y and Wolfbeis O S 2005 *Sensors Actuators B* **106** 369
- [5] Numata T and Otani Y 2007 *J. Mater. Sci.* **42** 1050
- [6] Chen L, Wang B and Wang G P 2006 *Appl. Phys. Lett.* **89** 243120
- [7] Maier S A, Andrews S R, Martín-Moreno L and García-Vidal F J 2006 *Phys. Rev. Lett.* **97** 176805
- [8] Jia F L, Yu C F, Ai Z H and Zhang L Z 2007 *Chem. Mater.* **19** 3648
- [9] Zhou H, Jin L and Xu W 2007 *Chin. Chem. Lett.* **18** 365
- [10] Dixon M C, Daniel T A, Hieda M, Smilgies D M, Chan M H W and Allara D L 2007 *Langmuir* **23** 2414
- [11] Koh H D, Kang N G and Lee J S 2007 *Langmuir* **23** 12817
- [12] Masuda H and Fukuda K 1995 *Science* **268** 1466
- [13] Choi D Y, Kim S H, Lee S M, Kim D S, Lee K H, Park H C and Hwang W B 2008 *Nanotechnology* **19** 145708
- [14] Xiao Z L *et al* 2002 *Appl. Phys. Lett.* **81** 2869
- [15] Masuda H, Yada K and Osaka A 1998 *Japan. J. Appl. Phys.* **37** L1340
- [16] Li Y B, Zheng M J, Ma L and Shen W Z 2006 *Nanotechnology* **17** 5101
- [17] Li Y B, Zheng M J and Ma L 2007 *Appl. Phys. Lett.* **90** 073109
- [18] Chu S Z, Wada K, Inoue S, Isogai M and Yasumori A 2005 *Adv. Mater.* **17** 2115
- [19] Lee W, Ji R, Gösele U and Nielsch K 2006 *Nat. Mater.* **5** 741
- [20] Huang L, Saito M, Miyagi M and Wada K 1993 *Appl. Opt.* **32** 2039
- [21] Xu W L, Chen H, Zheng M J, Ding G Q and Shen W Z 2006 *Opt. Mater.* **28** 1160
- [22] Fan D H, Ding G Q, Shen W Z and Zheng M J 2007 *Micropor. Mesopor. Mater.* **100** 154
- [23] Choi J, Luo Y, Wehrspohn R B, Hillebrand R, Schilling J and Gösele U 2003 *J. Appl. Phys.* **94** 4757
- [24] Liu K, Zhan L, Fan Z Y, Quan M Y, Luo S Y and Xia Y X 2007 *Opt. Commun.* **276** 8
- [25] Maarooof A I, Gentle A, Smith G B and Cortie M B 2007 *J. Phys. D: Appl. Phys.* **40** 5675
- [26] Martín-Moreno L, García-Vidal F J, Lezec H J, Pellerin K M, Thio T, Pendry J B and Ebbesen T W 2006 *Phys. Rev. Lett.* **86** 1114
- [27] Ghaemi H F, Thio T, Grupp D E, Lezec H J and Ebbesen T W 1998 *Phys. Rev. B* **58** 6779